Supplementary Material for: Large-Area Monolayer n-Type Molecular Semiconductors with Improved Thermal Stability and Charge Injection

Sai Jiang[1,], Lichao Peng[1], Xiaosong Du[1], Qinyong Dai[2], Jianhang Guo[2], Jianhui Gu[1], Jian Su[1], Ding Gu[1], Qijing Wang[2], Huafei Guo[1], Jianhua Qiu[1], and Yun Li[2,*]*

[1]School of Microelectronics and Control Engineering, Changzhou University, Changzhou, Jiangsu 213164, P. R. China.

[2]National Laboratory of Solid-State Microstructures, School of Electronic Science and Engineering, Collaborative Innovation Center of Advanced Microstructures, Nanjing University, Nanjing, Jiangsu 210093, P. R. China.

[#]These authors contribute equally.

[*]Corresponding authors: saijiang@cczu.edu.cn, yli@nju.edu.cn.

Experimental methods

Deposition of PDIF-CN_2 thin films and monolayer films. 50 nm-thick SiO_2/Si substrates were sequentially cleaned by sonication in acetone and isopropanol for 10 min. The n-type organic PDIF-CN_2 was used as semiconductors without further purification. PDIF-CN_2 was dissolved in anisole with a concentration of 0.1 wt%. 40 μL of PDIF-CN_2 solution was dropped onto a prepared SiO_2/Si substrate. The antisolvent of *N*,*N*-dimethylformamide (DMF) (40 μL) was drop-cast sequentially to cover the entire PDIF-CN_2 solution. Then, the solution was spin-coated at different speeds (1000 ~ 4000 rpm) for 60 s to obtain PDIF-CN_2 thin films and monolayer films.

Characterization of PDIF-CN_2 films. Optical microscopy images were taken using a Keyence VHX-5000 digital microscope. For regular AFM, the characterizations were performed on a Veeco Multimode 8 under ambient conditions. Raman spectroscopy was performed using a WITec Alpha 300R confocal Raman system with a 532 nm laser excitation (spot size ~ 300 nm, laser power 1 mW). photoluminescence spectroscopy was performed using a LabRAMHR800. A 325 nm laser was used as the excitation light source. The energy level was characterized by UPS (Thermo ESCALAB 250Xi, He−Iα = 21.2 eV).

Fabrications and electrical measurements of OFETs. For the fabrication of OFETs, monolayer PDIF-CN_2 films were first deposited on SiO_2/Si substrates. Evaporated Au

films under a deposition rate of 0.1 Å s^{-1} with a thickness of 100 nm were patterned into rectangle pads with an area of 80 μm × 100 μm. Two Au pads were subsequently transferred onto monolayer PDIF-CN_2 films for source and drain electrodes. Electrical measurements were carried out using an Agilent B1500 semiconductor parameter analyzer in a closed-cycle cryogenic probe station with a base pressure of 10^{-5} Torr.

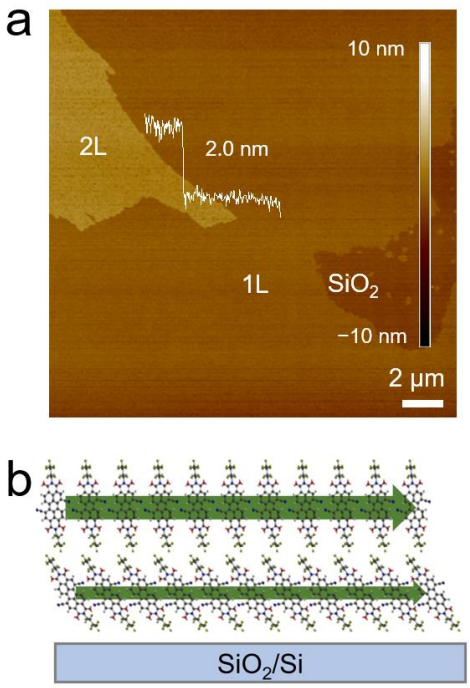

Figure S1. (a) The AFM image of bilayer PDIF-CN2 films, showing the thickness of the second molecular layer is 2.0 nm. (b) Schematic diagram of molecular packing of PDIF-CN_2 films.

Note 1. The GIXRD characterizations of PDIF-CN_2 films.

The crystallinity of the multilayer PDIF-CN_2 films before and after annealing was examined by the grazing incidence x-ray diffraction (GIXRD) (Figure S2). The monolayer films almost covered the SiO_2/Si substrate, while multilayer (2~4 layers) films can be found at the edge of the substrate using antisolvent-confined spin-coating method (Figure S2a). When the GIXRD was performed at the region of monolayer PDIF-CN_2 films, GIXRD results showed the complete absence of diffraction peaks due to the ultrathin property of the monolayer. Hence, the small-area multilayer films at the substrate edge were measured. The GIXRD results of the multilayer films after annealing showed the peaks with signals for the (*003*) and the (*004*) diffractions at 2θ = 16.3° and 2θ = 21.6°, respectively, while the absence of diffraction peaks was demonstrated in the spectra of the multilayer films before annealing (Figure R1b,c). [1,2] In addition, the absence of diffraction peaks of the (*001*) and (*002*) may

resulted from the weak signals from the first and second layers. The GIXRD results indicated that the multilayer PDIF-CN_2 films exhibited a crystalline property, and thermal annealing can effectively improve the crystallinity. Although GIXRD results showed the crystalline characteristics of multilayer films, it still cannot support the conclusion that it was a single-crystal feature of the monolayer films. Therefore, the high-quality property of the monolayer PDIF-CN_2 films was the large-area morphological uniformity.

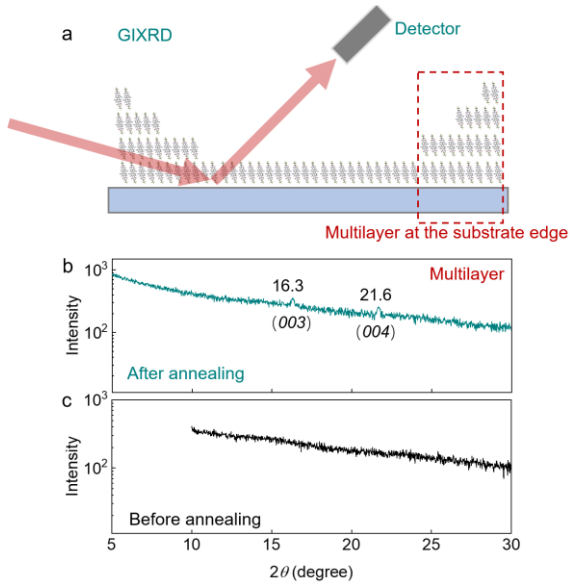

Figure S2. The GIXRD characterizations. (a) Schematic diagram of the measurement by GIXRD. The signals of multilayer PDIF-CN2 films at the edge of the substrate were detected. (b-c) GIXRD spectra of the multilayer PDIF-CN_2 films before (c) and after (b) annealing.

Note 2. The COMSOL Multiphysics simulation of the Marangoni flow.

We performed COMSOL Multiphysics simulations to study the Marangoni flow during the spin-coating process. The simulation geometry was shown in Figure S3. In the heterogeneous solvent system of DMF and anisole with vertical phase separation, DMF could be regarded as an additive solvent with 1 vol% for the main solvent of anisole with 99 vol%. The additive solvent of DMF could be considered as the species based on the transport of diluted species (TDS) model. Hence, the Multiphysics module with the TDS model and the laminar flow model was applied to the simulation.

In the laminar flow model, the solvent evaporates at the meniscus line (boundary 4) with a fixed mass flux of 0.001 kg m^{-2} s^{-1}. The surface tension coefficient for DMF was defined as $0.001 \cdot \left(\frac{c \cdot 73.09[g \cdot mol^{-1}]}{944000[g \cdot m^{-3}]} \cdot 1 \cdot 7.7 + 28.5\right)[\mathrm{N} \cdot m^{-1}]$.

In the TDS model, the diffusion coefficient (D_c) was 5×10^{-6} m^2 s^{-1}. The concentration of species (c) was 129.1 mol m^{-3} for DMF.

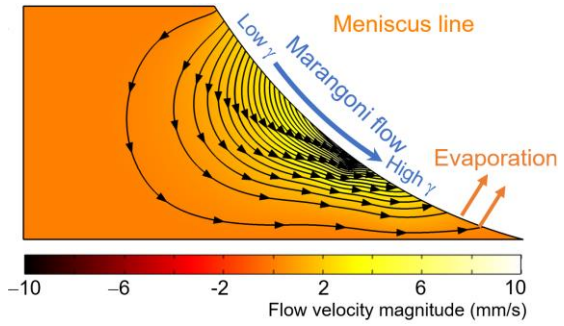

Figure S3. The COMSOL Multiphysics simulation of the Marangoni flow.

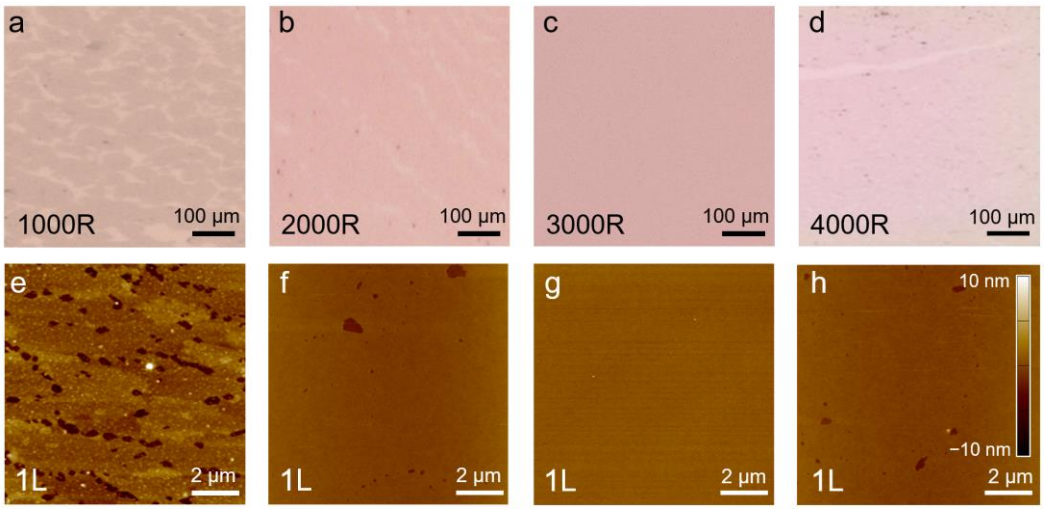

Figure S4. The film morphologies at different spin-coating speeds. (a-d) The optical microscopy images of monolayer PDIF-CN_2 films at 1000 rpm, 2000 rpm, 3000 rpm, and 4000 rpm, scale bar, 100 μm. (e-h) The AFM images of monolayer PDIF-CN_2 films at 1000 rpm, 2000 rpm, 3000 rpm, and 4000 rpm, scale bar, 2 μm.

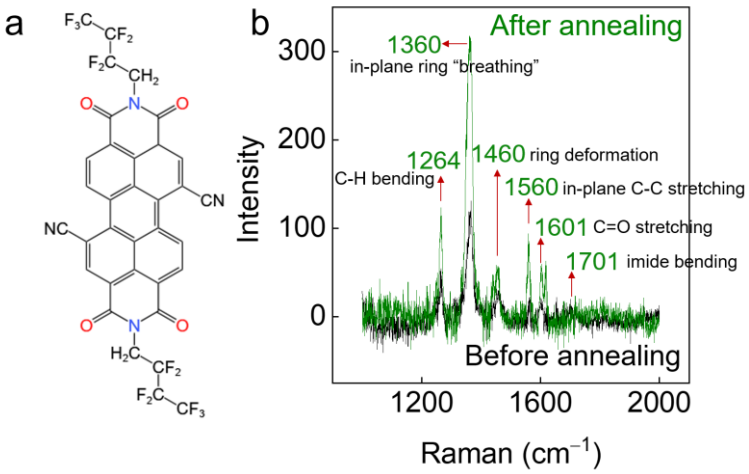

Figure S5. (a) Chemical structure of the organic semiconductor PDIF-CN_2. (b) Raman spectrum of monolayer PDIF-CN_2 films on SiO_2 before and after annealing.

As shown in Figure S5, the characteristic signals of the monolayer PDIF-CN_2 spectrum can be measured at: 1264 cm^{-1} (C–H bending), 1360 cm^{-1} (in-plane ring "breathing"), 1460 cm^{-1} (ring deformation), 1560 cm^{-1} (in-plane C–C stretching), 1601 cm^{-1} (C=C stretching), and 1701 cm^{-1} (imide bending). [3,4] Additional signals originating from the side chains of the PDI were commonly larger than 2000 cm^{-1}, which were not detected in our experiment. The measured characteristic signals were close to the Raman spectrum of PDI. [3] In addition, the Raman peak intensity at 1360 cm^{-1} of the monolayer films after annealing was three times higher than its pre-annealing value, and the full width at half maximum (FWHM) of Raman peaks was smaller than the pre-annealing films, both supporting the significant improvement of the film crystallinity and reduction of defects by annealing.

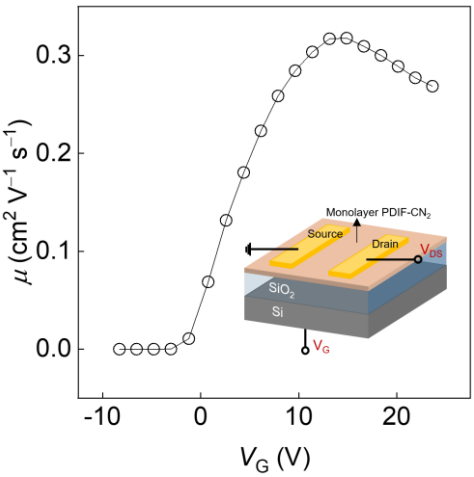

Figure S6. The electron mobility as a function of the gate voltage. The inset is a typical diagram of a monolayer-based transistor.

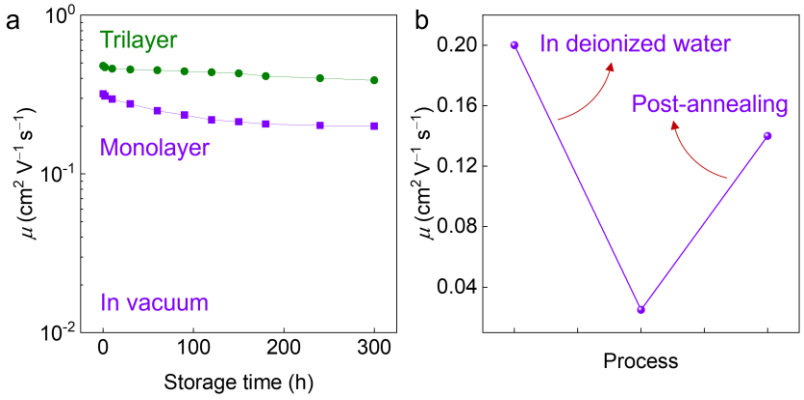

Figure S7. (a) The mobility stability of the monolayer and trilayer-based transistors stored in vacuum. (b) A post-annealing treatment at 120 ℃ for 20 min under vacuum conditions could restore the electrical performance to approach the origin mobility values.

Note 3. UPS and electrical performance of multilayer PDIF-CN_2 films.

The inclined drop-cast method was used to deposit multilayer PDIF-CN_2 films. First, PDIF-CN_2 was dissolved in anisole with a concentration of 0.1 wt%. After the solute was fully dissolved, we pipetted 50 μl from the PDIF-CN_2 solution and mixed it with 200 μl of DMF solvent. Then, 5 μL of the mixed solution was dropped onto a prepared SiO_2/Si substrate, which was inclined on the substrate (Figure S6a). As the droplet gradually slides over the inclined SiO_2/Si substrate, multilayer PDIF-CN_2 films can be deposited with a large area (Figure S8b).

The multilayer PDIF-CN_2 films for the UPS characterizations were deposited by the inclined drop-cast method (Figure R4). The obtained films exhibited multilayer features on the centimeter-sized SiO_2/Si substrate including large-area bilayer (2L) films, trilayer (3L) films, and some thicker crystalline films and islands. In the UPS characterizations, the size of the light spot was 3 mm × 3 mm, containing most of the 3L films. Therefore, the thickness of multilayer in the UPS data can be regarded as trilayer films (~ 3L) over the millimeter-sized scale.

For comparison, we further reduced the coverages of the 3L and thicker films by increase the tilt angle of the SiO_2/Si substrate to obtain large-area bilayer films using the inclined drop-cast method. Although trilayer and thicker films still existed, we approximated that the thin film obtained is a bilayer (~ 2L). UPS and PL characterizations were performed on the bilayer films. When the film thickness was varied from ~ 3L to ~ 2L, the energy levels were almost unchanged. Hence, the decrease of the film thickness was not the reason for the energy level shifts.

The energy level shifts can be found when the films decrease to the monolayer. Such an abrupt transition may be attributed to strong modulation of the molecular packing by interfacial vdW interactions. As shown in Figure S1b, the molecules of 1L films were more tilted on the substrate than that of 2L molecules due to the stronger molecule–substrate interactions, which led to weaker π-π stacking between molecules in monolayer films. [5] The different molecular packing had important influences on the molecular orbitals in 1L and 2L films, which could result in the energy level shifts. [5,6] Therefore, the coupling between substrate and molecules might be the reason for the energy level shifts.

We further fabricated an OFET with trilayer (3L) PDIF-CN_2 films to study the electrical properties. An obvious nonlinear increase of output characteristic can be found from V_{DS} of 0 V to 5 V, which indicated a larger contact resistance between Au and 3L PDIF-CN_2 films compared with monolayer films (Figure S7a,b).

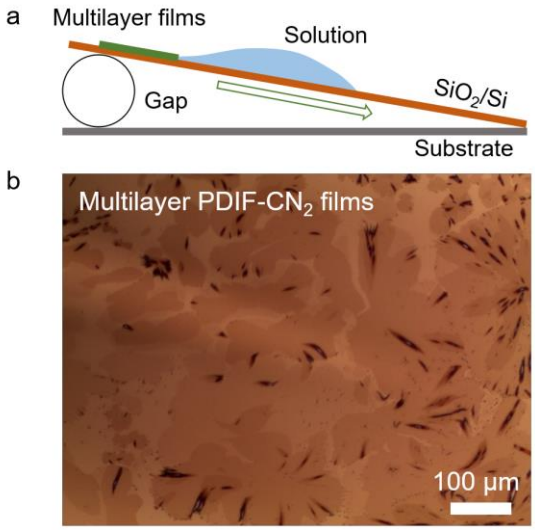

Figure S8. The multilayer PDIF-CN_2 films deposited by an inclined drop-cast method. (a) The schematic of the inclined drop-cast method. (b) The optical image of deposited multilayer PDIF-CN_2 films, scale bar, 100 μm.

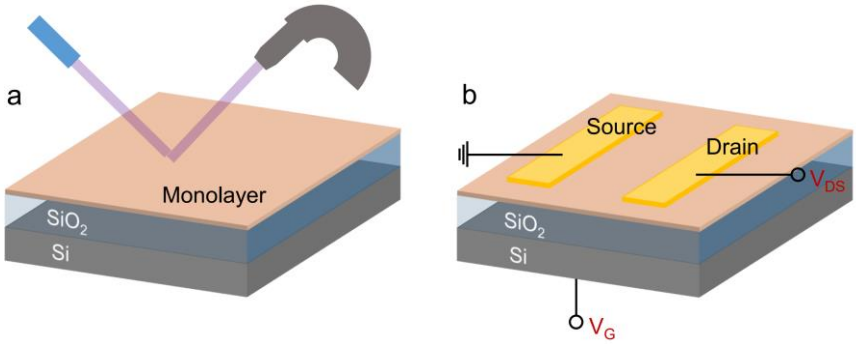

Figure S9. (a) The schematics of the characterizations of UPS on monolayer films. (b) The schematics of the transistor with monolayer films as conducting channel.

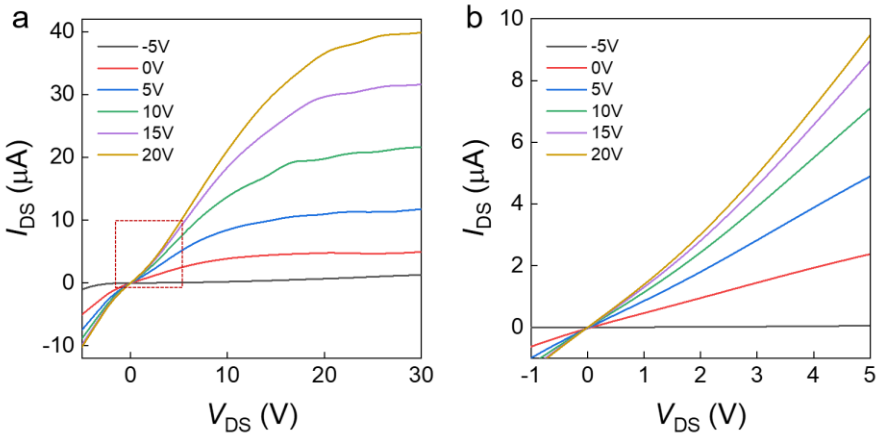

Figure S10. (a) Output characteristics of the OFET with multilayer PDIF-CN_2 films at gate voltage from −5 to 20 V. (b) Nonlinear output curves at small V_{DS} from 0 to 5 V corresponding to output characteristic of (a).

References:

[1] F. Chiarella, T. Toccoli, M. Barra, L. Aversa, F. Ciccullo, R. Tatti, R. Verucchi, S. Iannotta, and A. Cassinese, *High Mobility n -Type Organic Thin-Film Transistors Deposited at Room Temperature by Supersonic Molecular Beam Deposition*, Appl. Phys. Lett. **104**, 143302 (2014).

[2] B. A. Jones, A. Facchetti, M. R. Wasielewski, and T. J. Marks, *Tuning Orbital Energetics in Arylene Diimide Semiconductors. Materials Design for Ambient Stability of n-Type Charge Transport*, J. Am. Chem. Soc. **129**, 15259 (2007).

[3] G. Abellán, V. Lloret, U. Mundloch, M. Marcia, C. Neiss, A. Görling, M. Varela, F. Hauke, and A. Hirsch, *Noncovalent Functionalization of Black Phosphorus*, Angew. Chemie **128**, 14777 (2016).

[4] A. Łapiński, A. Graja, I. Olejniczak, A. Bogucki, M. Połomska, J. Baffreau, L. Perrin, S. Leroy-Lhez, and P. Hudhomme, *Vibrational and Electronic Properties of Perylenediimide Linked to Fullerene and Tetrathiafulvalene*, Mol. Cryst. Liq. Cryst. **447**, 87 (2006).

[5] Y. Zhang, J. Qiao, S. Gao, F. Hu, D. He, B. Wu, Z. Yang, B. Xu, Y. Li, Y. Shi, W. Ji, P. Wang, X. Wang, M. Xiao, H. Xu, J. Bin Xu, and X. Wang, *Probing Carrier Transport and Structure-Property Relationship of Highly Ordered Organic Semiconductors at the Two-Dimensional Limit*, Phys. Rev. Lett. **116**, 016602 (2016).

[6] D. He, J. Qiao, L. Zhang, J. Wang, T. Lan, J. Qian, Y. Li, Y. Shi, Y. Chai, W. Lan, L. K. Ono, Y. Qi, J. Bin Xu, W. Ji, and X. Wang, *Ultrahigh Mobility and Efficient Charge Injection in Monolayer Organic Thin-Film Transistors on Boron Nitride*, Sci. Adv. **3**, 1 (2017).